Soil type affects not only magnitude but also thermal sensitivity of N_2O emissions in subtropical mountain area

Bowen Zhang[1,2], Minghua Zhou[1*], Bo Zhu[1]， Qianying Xiao[1,2], Tao Wang[1], Jialiang Tang[1], Zhisheng Yao[3], Ralf Kiese[4], Klaus Butterbach-Bahl[4], Nicolas Brüggemann[5]

[1] Key Laboratory of Mountain Surface Processes and Ecological Regulation, Institute of Mountain Hazards and Environment, Chinese Academy of Sciences, Chengdu 610041, PR China

[2] University of Chinese Academy of Sciences, Beijing 100049, PR China

[3] State Key Laboratory of Atmospheric Boundary Layer Physics and Atmospheric Chemistry, Institute of Atmospheric Physics, Chinese Academy of Sciences, Beijing 100029, PR China

[4] Institute for Meteorology and Climate Research (IMK-IFU), Karlsruhe Institute of Technology, Kreuzeckbahnstr. 19, 82467 Garmisch-Partenkirchen, Germany

[5] Institute of Bio- and Geosciences - Agrosphere (IBG-3), Forschungszentrum Jülich GmbH, 52425 Jülich, Germany

*** Corresponding author**

Minghua Zhou

Phone: +86-28-85570461

E-mail: mhuazhou@imde.ac.cn

Address: No.9, Fourth Section, Renminnanlu Road,Wuhou District, 610041 Chengdu, China.

Abstract

It is a concern whether the effect of soil type on N_2O emissions has to be considered for regional mitigation strategies and emission estimates in mountainous areas with inherent spatial heterogeneities of soil type. To date, there were few field experiments which investigated soil type effects on N_2O emissions. Thus a 2-year field study was conducted to measure N_2O emissions and soil environmental variables from three different soils that were formed from similar parental rock under the same climate. Seasonal N_2O fluxes ranged from 0.18 to 0.40 kg N ha^{-1} for wheat seasons and 0.40 to 1.50 kg N ha^{-1} for maize seasons across different experimental soils. The intra- and inter-annual variations in N_2O emissions were mainly triggered by temporal dynamics of soil temperature and moisture conditions. On average, seasonal N_2O fluxes for acidic soils were significantly lower than for neutral and alkaline soils in cold-dry wheat seasons while significantly greater than for neutral and alkaline soils in warm-wet maize seasons. These determined differences of N_2O emissions were mainly caused by differences of initial soil properties across different soils. Moreover, seasonal N_2O fluxes were positively correlated with soil pH in wheat seasons, but negatively correlated in maize seasons. The temperature sensitivity coefficient (Q_{10}) of soil N_2O emissions for acidic soil (4.06) were significantly greater than those for neutral (1.82) and alkaline (1.15) soils. Overall, N_2O emissions for acidic soils were not only higher than those for neutral and alkaline soils but also more sensitive to changing temperature. The present study highlights that soil type is needed to be carefully considered for regional estimate and proposing mitigation strategy of N_2O emissions especially in subtropical mountain regions with inherent great heterogeneity of soil type.

Keywords: N_2O emission, soil type, subtropical mountain area, temperature sensitivity

1. Introduction

N_2O emissions from agricultural soils account for approximately 60% of total global anthropogenic emissions (IPCC, 2014). However, these estimates have high uncertainties due to substantial spatial-temporal variations across different soil types, climates, and management practices (Shcherbak et al., 2014; Zhou et al., 2018; Wang et al., 2018). For example, previous studies have demonstrated that disregarding heterogeneities in soil type and the associated spatial disparities of N_2O emission may largely account for the uncertainties in regional and global N_2O emission estimates (Paustian et al., 2016). Recently, a global meta-analysis indicates that IPCC-Tier 1 estimates could lead to deviations of -75% and 35% for acidic and alkaline soils respectively when ignoring the soil pH effects on regional and global N_2O budgets (Wang et al., 2018). Although the scientific community began to evaluate effects of soil type on N_2O emissions but mainly through laboratory incubation experiment and short-term field experiment (Chirinda et al., 2010; Pelster et al., 2012), there were few multi-year field study to assess effects of soil type on N_2O emissions under same climate and agricultural management practice.

Soil N_2O is the intermediate product of soil biotic and abiotic N transformation processes that occur simultaneously in soils (Butterbach-Bahl et al., 2013; Heil et al., 2015). These N transformation processes and associated soil N_2O emissions are not only controlled by the availabilities of C and N substrates but also by other soil properties (Skiba and Ball, 2002; Butterbach-Bahl et al., 2013; Zhou et al., 2017b). For example, several previous studies have demonstrated that soil pH is the key factor of soil N_2O emissions

(Bakken et al., 2012; Shaaban et al., 2018; Wang et al., 2018). Low soil pH generally decreases the activity of the *nosZ* genes (Shaaban et al., 2018) and constrains the assembly of functional N_2O reductase, thereby increasing the ratio of N_2O:N_2 during denitrification (Bakken et al., 2012). Likewise, previous field and laboratory studies also observed decreases in N_2O emissions from forest and agricultural soils due to a pH increase after liming and/or biochar additions (Borken and Brumme, 1997; Obia et al., 2015). However, N_2O emissions may increase with an increase of soil pH because high pH can enhance the N_2O production processes of nitrification and dissimilatory nitrate reduction to ammonium (DNRA) (Stevens et al., 1998; Zhu et al., 2019). Thus, the response of N_2O emissions to soil pH remains uncertain.

In addition to soil pH, soil texture through regulating soil gas diffusivity and thereby the availability of oxygen (O_2) in soils could control soil N_2O production-consumption processes as well as diffusion-emission processes (Gu et al., 2007; Butterbach-Bahl et al., 2013; Zhou et al., 2017b). For example, Mctaggart et al., (2002) found that N_2O flux was negatively correlated with soil gas diffusivity of Japanese upland soils, and Pilegaard et al. (2013) reported that the optimal soil water-filled pore space (WFPS) for N_2O emissions from sandy loam soil is much higher than that for sandy clay loam soil.

Numerous studies have stated that soil moisture and temperature are key regulators of soil N_2O emissions (Butterbach-Bahl et al., 2013; Pilegaard, 2013). For example, Davidson et al. (1993) found that soil N_2O emissions have optimum soil moisture conditions of 70-80% WFPS. Soil temperature can affect soil N_2O emissions through regulating enzymatic activity, chemical nitrogen turnover rate, and gas diffusion process (Skiba and Ball, 2002; Butterbach-Bahl et al., 2013; Zhang et al., 2020). The temperature sensitivity (Q_{10}) of N_2O

93 emissions is commonly defined as the factor by which N_2O emissions increase with a 10 °C
94 rise in temperature (Schindlbacher et al., 2004; Zhou et al., 2018). However, soil substrate
95 availability, microbial community composition and biomass, enzymatic activities, and soil
96 porosity change with soil types (Rowlings et al., 2012; Gu et al., 2013), which might result
97 in different Q_{10} values of N_2O emissions in different soil types. Previous studies have
98 reported Q_{10} values of N_2O emissions even greater than the global mean Q_{10} values of soil
99 CO_2 emissions (mean: 3.0) (Schindlbacher et al., 2004; Parkin and Kaspar, 2006; Zhou et
100 al., 2018). Thus, direct quantification of the Q_{10} values of soil N_2O emissions via field
101 measurements is necessary.

102 To improve the accuracy of N_2O emission estimates in the subtropical and tropical
103 ecosystems, intensive field N_2O emission measurements have been conducted over the last
104 decade (Liu et al., 2017b). However, the accuracy of regional and global N_2O emission
105 estimates still has been constrained likely by that soil type variability has previously been
106 disregarded (Paustian et al., 2016), especially in the mountainous regions with great
107 regional heterogeneities of soil type. To date, the multi-year field studies to investigate
108 effects of soil type on N_2O emissions and the underlying mechanisms in subtropical
109 agricultural soils are still limited. Therefore, we conducted a 2-year consecutive field study
110 to simultaneously measure N_2O emissions as well as soil environmental variables and
111 agronomical performances from three different agricultural soils in a subtropical
112 mountainous landscape under identical climate and agricultural management practice. The
113 aim of this study was therefore to quantify the effect of soil type on N_2O emissions thereby
114 exploring the main regulators. We expect to clarify the concern whether role of soil type in
115 N_2O emissions was necessary to be considered when one proposes regional mitigation

strategy and estimates regional emission of N_2O in mountainous area, where substantial spatial heterogeneity of soil type is the inherent property.

2. Materials and methods

2.1 Site description and experimental design

The field experiment was conducted at Yanting Agro-Ecological station of the Chinese Academy of Sciences (31°16' N, 105°28' E) in Southwest China. The climate is classified as a moderate subtropical monsoon climate with mean annual precipitation of 863 mm and mean annual air temperature of 17.3 °C over the last 3 decades (1990-2019).

The field experiment included three types of soil, i.e. acidic soil (AC, pH 5.09), neutral soil (NE, pH 6.75), and alkaline soil (AL, pH 8.37). The soils were all formulated from the similar parental bedrock of purplish sandstone (Table S1) and characterized by rapid weathering, i.e. the weathering and soil formulation process is mostly taken less than 50 years (Zhu et al., 2008). The three soils are classified as Eutric Regosol in accordance with the FAO Soil Classification. They are the main agricultural soil types in mountain area of the Upper Yangtze River watershed with distribution area of over 300 000 km^2 and feeding more than 10% of the Chinese population. For each soil type, three replicate field plots were established and randomly distributed. Each field experimental plot with a size of 7.5 m^2 (5 m × 1.5 m) is hydrologically isolated with partition walls of cement. The partition walls were constructed at least 60 cm into the bedrock for avoiding the horizontal seepage flow to other plots. The chemical-physical properties of the topsoil (0–20 cm) are shown in Table 1.

All experimental plots were cultivated with the same winter wheat–summer maize

rotation system and the same agricultural management practices since 2012. Briefly, ammonium carbonate (130 kg N ha^{-1} for the wheat season and 150 kg N ha^{-1} for the maize season), superphosphate (90 kg P_2O_5 ha^{-1}), and potassium chloride (36 kg K_2O ha^{-1}) were distributed and manually mixed into the surface soil layer (e.g., approximately 10–15 cm) in accordance with local management practices. The fertilizer application rates were based on local recommendations (Zhou et al., 2014). Winter wheat (*Triticum aestivum*) was sown in November and harvested in the following early May, and summer maize (*Zea mays L.*) was sown with 0.45 m row spacing and 0.3 m plant spacing in late May and harvested in September.

2.2 Measurements of N_2O emissions

The soil N_2O emission measurements in the present study were conducted from October 2017 to September of 2019 (i.e. starting 5 years after the experimental plots had been established) by using the static chamber-gas chromatography technique (Zheng *et al.*, 2008; Zhou *et al.*, 2014). Stainless steel square chamber bases (50 cm × 50 cm) were pre-installed in the soil to a depth of 15 cm at each plot after basal fertilization and kept undisturbed throughout each cropping season. There was a groove (width and depth: 3 cm each) on top of each chamber base, used as water seal during chamber measurement. Stainless steel chambers (50 cm × 50 cm × 50 cm) were wrapped with a thermal insulation layer to minimize air temperature variations inside the chamber during the measurements. In addition, each chamber was equipped with two fans (10 cm diameter) to mix the headspace air, and a thermometer to measure the air temperature. To minimize the disturbance of experimental plots by measurement and sampling activities, a wooden

walking board was setup at each plot before each cropping season.

The gas sampling was performed daily for the first week, and every other day for the second week following N fertilization, and then changed to twice per week throughout each cropping season. For each measurement, five gas samples were taken between 09:00 and 11:00 a. m., in 8-min intervals (0, 8, 16, 24, and 32 min after chamber closure) from the headspace of each chamber using 60-ml gas-tight syringes. All gas samples were analyzed within 8 h using a gas chromatograph (Agilent 7890-B, USA) equipped with an electron capture detector for N_2O analysis. The carrier gas flow, column oven temperature, and flame ionization detector were periodically calibrated based on the GC calibration protocol. Standards were run periodically throughout the sample run, i.e. for every 5 samples, the N_2O concentrations were calibrated using a reference gas with standard N_2O concentration (0.49ppmv, Chengdu Chenggang Messer Gas Products, Co., Ltd, Chengdu, China) (Parkin and Venterea, 2018). N_2O fluxes were calculated based on the change rate of N_2O concentration in the enclosed chamber headspace over time (correlation coefficients > 0.95), as described by Zheng et al. (2008). The cumulative N_2O emissions were calculated by linear interpolation of the daily fluxes between gas sampling dates (Parkin and Venterea, 2018).

2.3 Auxiliary measurements

Soil samples were collected from each plot using a soil auger after each gas sampling, and the visible stones, roots, and other litters were removed manually before mixing completely. The mixed samples were then extracted with 2M KCl solution (soil: solution =1:5 w/v), shaken for 1 h, and filtered through 0.45-μm polyethersulfone membrane

(Whatman@) filter. The extracts were analyzed for NH_4^+, NO_3^- and NO_2^- content using continuous flow analyzer (Auto Analyzer 3, SEAL Analytical, Germany). Soil dissolved organic carbon (DOC) was extracted with deionized water (soil: water =1:5 w/v), shaken for 1h then centrifuged for 10 min at 4,000 rpm. The supernatant was filtered through 0.45-μm polyethersulfone membrane (Whatman@) and analyzed using a continuous flow analyzer equipped with a chemical oxidation module (Auto Analyzer 3, SEAL Analytical, Germany). Soil clay mineral contents were measured by a multipurpose X-ray diffraction system (Ultima IV, Rigaku, Japan). Daily precipitation and air temperature were recorded by established automatic meteorological stations that is about 100 m from the experimental plots. The temperature and moisture content of the topsoil (0–5 cm) were monitored with a manual thermometer (JM624, Jinming Instrument Co. Ltd, Tianjin, China) and a portable frequency domain reflector probe (MP-406B, Zhongtian Precision Instruments Co. Ltd, Nantong, Jiangsu, China), respectively. The measured volumetric moisture was converted to WFPS (%) according to the following equation:

$$WFPS(\%) = V / [1 - (BD / 2.65)] \times 100\% \quad (1)$$

where V is the soil volumetric moisture measured at each plot and BD is the soil bulk density.

The classic exponential regression equation was used to calculate the relationship between soil temperature and N_2O emissions, which was fitted according to equation (2), where E_{N2O} is soil N_2O emission rate, a and b are fitted parameters, and T is soil temperature.

$$E_{N2O} = a \times \exp^{bT} \quad (2)$$

The Q_{10} value was calculated by the following equation:

$$Q_{10} = \exp^{10 \times b} \quad (3)$$

After crop maturation, the whole plant biomass of wheat and maize was harvested from each plot and separated into root, straw, and grain parts, and then air-dried and weighed for subsequent crop yield calculation. A subsample of root, straw, and grain parts was prepared and oven-dried to constant weight at 75 °C then ground for total nitrogen content analysis with an elemental analyzer (Vario MACRO cube, Elementar, Analysensysteme GmbH, Langenselbold, Germany). Plant N uptake (kg N ha^{-1}) was calculated by the following equation:

$$Plant\ N\ uptake\left(kg\ N\ ha^{-1}\right) = plant\ dry\ matter\ biomass \times plant\ N\ content \quad (4)$$

and the yield-scaled N_2O emission intensity (g N Mg^{-1}) was calculated with the equation:

$$Yield-scaled\ N_2O\ emissions\ \left(g\ N\ Mg^{-1}\right) = seasonal\ fluxes / grain\ yield \quad (5)$$

2.4 Functional gene abundance

Soil samples for functional gene abundance analysis were taken following the maize harvest in September 2018, then stored in liquid nitrogen. The corresponding primer sequences are listed in Supplementary Table S2. Briefly, 0.5 g of fresh soil was extracted using the FastDNA spin kit according to the product instructions (MP Biomedicals, CA, USA). The quality of extracted DNA was analyzed using gel electrophoresis (0.8% agarose). The nitrification-related (ammonia oxidizing archaea (AOA) *amoA*, ammonia oxidizing bacteria (AOB) *amoA*, *hao*) and denitrification-related (*narG, napA, nirS, nirK, norB, nosZ*) functional genes were amplified with quantitative real-time polymerase chain reaction (PCR) (TIB8600, Triplex International Biosciences Co., Ltd, China). A standard curve was prepared with plasmid DNA from one representative clone containing each target gene. Each reaction mixture (16 μl) included 10 μl of 2×SYBR real-time PCR pre-

mixture, 0.4μl each of forward and reverse primers, and 1 μl of DNA template containing approximately 10 ng of DNA. PCR reactions were performed according to the following program: 95 °C for 5 min for 40 cycles (95 °C for 15 s, 60 °C for 30 s).

2.5 Statistical analysis

All statistical analyses were performed using SPSS 24.0 software (SPSS Inc., 2016). Soil properties, seasonal and annual N_2O fluxes, grain yield, plant N uptake, yield-scaled N_2O emissions, and functional gene abundance were tested for significant differences by the least significant difference at the $p<0.05$ level with one-way ANOVA following the Tukey's multiple range test. Sources of variance were analyzed by univariate analysis. Significant differences among soils in the box-whisker plots were compared by the least significant difference at the $p<0.05$ level with one-way ANOVA followed by the post-hoc LSD test. The relationships between normalized N_2O fluxes and soil variables (NH_4^+, NO_3^-, NO_2^-, DOC, soil temperature, and WFPS) were explored using multiple linear regression analysis. Moreover, the relationships between daily N_2O emissions and soil temperature and between seasonal or annual N_2O fluxes and soil pH were explored using nonlinear regression. Figures were prepared using Origin 9.4 software (Origin Lab Corporation, Northampton, USA).

3. Results

3.1 Environmental conditions and crop productivity

Throughout the experimental period, average soil and air temperatures were 17.7 °C and 16.4 °C, respectively (Fig. 1a). The mean annual precipitation was 858.4 mm, while

the precipitation during the maize growing season in 2019 (809 mm) was approximately twice as high as for 2018 (418mm) (Fig. 1b). Soil WFPS was in the range of 7.49% to 67.11% (mean: 34.52%). There were no significant differences in soil temperature or moisture content between the different soils in either maize or wheat season (Fig. 2a-b).

The average soil NH_4^+ concentrations varied significantly between the different soils in following order: AC (113.35 mg N kg^{-1}) > NE (54.48 mg N kg^{-1}) > AL (31.15 mg N kg^{-1}) (p<0.05) (Fig. 2c). The mean soil NO_3^- concentrations for AC (28.6 mg N kg^{-1}) and AL (30.59 mg N kg^{-1}) soils were significantly greater than those for NE soil (20.09 mg N kg^{-1}) (p<0.05) (Fig. 2d). Soil NO_3^- increased following fertilization then declined gradually, but with different patterns for different soils (Fig. 3b). The soil NO_2^- concentrations for AL soil (0.03–31.10 mg N kg^{-1}) were significantly higher than those for AC (0.01–2.5 mg N kg^{-1}) and NE (0.01–1.52 mg N kg^{-1}) soils (Fig. 3e). The average soil DOC concentrations for NE (45.70 mg C kg^{-1}) soil were significantly greater than those for AC (30.62 mg C kg^{-1}) and AL (32.03 mg C kg^{-1}) soils (Fig. 3d).

Crop yields and plant N uptake in the wheat and maize season were significantly affected by the soil type and year × soil type interaction (except for plant N uptake in the wheat season), however, no effects were detected for the year alone (Table 2). Crop yields were 2.57–3.32 Mg ha^{-1} for the wheat season and 3.28–5.67 Mg ha^{-1} for the maize season. NE soil showed the best yield performances, which were11.6%–59.8% and 1.2%–27.7% higher than those of AC and AL soils, respectively. The plant N uptake was 73.48–102.18 kg N ha^{-1} for the wheat season and 96.68–140.22 kg N ha^{-1} for the maize season. Compared to the 2018 maize season, plant N uptake was significantly higher by 41.55% in AC soil but lower by 14.75% in AL soil in the 2019 maize season (p < 0.05), respectively.

277

278 *3.2 Soil N_2O emissions*

279 Soil N_2O emissions exhibited significantly different dynamics between the different
280 experimental soils (Figs. 3e and 4). Across different experimental years and soils, the soil
281 N_2O emissions ranged from -4.35 to 20.27 μg N m^{-2} h^{-1} for AC, -10.74 to 34.03 μg N m^{-2}
282 h^{-1} for NE and -2.17 to 43.40 μg N m^{-2} h^{-1} for AL. The soil N_2O emissions were
283 significantly higher in the maize season compared to the wheat season, which were in the
284 range of 1.11 to 228.86 μg N m^{-2} hr^{-1} for AC, -0.50 to 45.87 μg N m^{-2} hr^{-1} for NE and -
285 10.47 to 171.65 μg N m^{-2} hr^{-1} for AL in the maize season. The N_2O emissions from AC,
286 NE and AL soils peaked on average 35.5, 19.5, and 13.0 days after fertilization in the wheat
287 season, and 32.5, 18.0, and 4.0 days in the maize season, respectively.

288 N_2O fluxes in the wheat season were significantly affected by the factors of soil type,
289 year, and year × soil type (p<0.05), whereas in the maize season or on the annual scale the
290 factors year or year × soil type factor had no effect on N_2O fluxes (Table 2). Seasonal N_2O
291 fluxes ranged from 0.18 to 0.40 kg N ha^{-1} for the wheat season and 0.40 to 1.50 kg N ha^{-1}
292 for the maize season across all experimental soils. The average annual N_2O fluxes were
293 1.52 kg N ha^{-1} for AC soil, 0.67 kg N ha^{-1} for NE soil, and 0.78 kg N ha^{-1} for AL soil. The
294 N_2O emission pulses due to fertilization events significantly contributed to cumulative N_2O
295 emissions in the maize season (81.84% for AC, 54.12% for NE, and 65.14% for AL);
296 however, nonsignificant contributions of these pulses were observed during the wheat
297 season (Fig. 3e). The maize season averagely accounted for 55.0%, 63.1% and 84.6% of
298 annual N_2O fluxes for AL, NE and AC soils, respectively, throughout the experimental
299 period (Fig. 4).

Yield-scaled N_2O emissions reflect both the crop yield and environmental performance of different soils with regard to N_2O emissions (Table 2). The annual yield-scaled N_2O emissions were in the range of 132.1–581.3 g N_2O-N Mg^{-1} yield, across different years and soils. The average yield-scaled N_2O emissions for AC, NE, and AL soils, respectively, were 82.63, 77.00, and 119.00 g N_2O-N Mg^{-1} yield for the wheat season and 346.96, 76.10, and 88.70 g N_2O-N Mg^{-1} yield for the maize season. Compared with the wheat season, yield-scaled N_2O emissions of the maize season were on average 407.6% higher for the AC soil, 25.0% lower for the AL soil. Yield-scaled N_2O emissions of the NE soil showed inter-annual variability in the maize and wheat seasons.

3.3 Functional gene abundance

As shown in Fig. 5, there were significant differences in the abundance of N_2O-forming and N_2O-reducing functional genes among the three soils. Regarding the nitrification process, the abundance of functional genes ranged from 7.53×10^5 to 1.91×10^7 copies g^{-1} soil for the AOA *amoA* gene, 2.76×10^6 to 1.65×10^7 copies g^{-1} soil for the AOB *amoA* gene, and 1.38×10^8 to 5.05×10^8 copies g^{-1} soil for the *hao* gene, (Fig. 5a). The abundance of AOA *amoA*, AOB *amoA* and *hao* genes was significantly and positively correlated with soil pH, but not significantly affected by other soil properties (Table S5).

Nitrate-reducing microorganisms were evaluated by quantifying the abundance of *narG* and *napA* genes, which ranged from 5.88×10^5 to 7.17×10^5 copies g^{-1} soil and 7.64×10^4 to 4.29×10^5 copies g^{-1} soil across the experimental soils, respectively (Fig. 5b). No significant differences were observed in *narG* gene abundance among the three soils, whereas the gene abundance of *napA* was significantly and positively correlated with soil pH (Table S5). The nitrite-reducing bacteria functional gene abundances of *nirS* (3.01×10^5

to 1.09×10^6 copies g^{-1} soil) and *nirK* (5.14×10^3 to 4.22×10^4 copies g^{-1} soil) showed significant differences ($p<0.05$) among the soils, i.e., AL>NE>AC. Gene copies of the nitrous oxide reducing functional gene *nosZ* were lowest in AC soil (7.91×10^4 copies g^{-1} soil), followed by AL soil (1.81×10^5 copies g^{-1} soil) and NE soil (5.91×10^5 copies g^{-1} soil).

3.4 Correlations between soil N_2O emissions and environmental factors

Soil N_2O emissions were mainly affected by soil temperature, WFPS, mineral N substrate (NH_4^+, NO_3^-, NO_2^-), and DOC content across the different experimental years and soils (Table S3). The linear regression model of these environmental factors explains daily N_2O emission variations of 9.0%–15.0% in the wheat season, 27.0%–51.0% in the maize season, and 26.0%–49.0% on the annual scale (Table 3). Across the three soils, the exponential relationship between N_2O fluxes and soil pH was found positive ($p < 0.01$) in the wheat season while negative in the maize season or on the year-round scale. (Fig. 7). Soil N_2O emissions increased exponentially with soil temperature in the three soils, exhibiting Q_{10} values of 4.06, 1.82, and 1.15 for AC, NE, and AL soils, respectively (Fig. 6).

4 Discussion

4.1 Soil type and N_2O emissions

In the present study, the average seasonal N_2O fluxes were 0.28 kg N ha^{-1} $season^{-1}$ for wheat and 0.71 kg N ha^{-1} $season^{-1}$ for maize (Table 2). Our observations fall within the range of previously reported N_2O emissions for wheat and maize systems whereas the mean values are both lower than the global averages of 1.44 kg N ha^{-1} $season^{-1}$ and 3.01 kg N ha^{-}

346 ^{1} season^{-1} for wheat and maize systems, respectively (Linquist et al., 2012). In addition, the
347 intra- and inter-annual dynamics of soil N_2O emissions were also observed in this study
348 (Fig. 3, Table 2), although under same agricultural management practices and
349 environmental conditions. Previous studies have effectively documented that the dynamics
350 of soil environmental variables are the main drivers of soil N_2O emissions variation in
351 various ecosystems (Luo et al., 2012; Rowlings et al., 2012; Zhou et al., 2017a). In this
352 study, soil moisture conditions (WPFS) were positively correlated with N_2O emissions
353 (Table 3), suggesting that rainfall dynamics likely contribute to temporal variations of N_2O
354 emissions. Nevertheless, the current study indicates that rainfall events do not always
355 induce high pulses of N_2O emissions (Fig. 3), which contrasts with previous findings of
356 rainfall events as triggers of hot moments of N_2O emission (Yao et al., 2015; Song et al.,
357 2019; Shang et al., 2020). Pulses of soil N_2O emissions were only observed after large
358 rainfall events in combination with N fertilization events in maize seasons and not after
359 rainfall events in wheat seasons (Fig. 3). The lack of N_2O pulses after rainfall events in the
360 wheat season was most likely due to nitrification-denitrification processes being hindered
361 by low soil temperature (Szukics et al., 2010; Butterbach-Bahl et al., 2013). The absence
362 of soil N_2O emission pulses after rainfall events during July to September (maize season)
363 could be explained with NO_3^- limitation (Table 2, Fig. 3) because high NO_3^- leaching loss
364 often occurs after large rainfall events thereby decreasing soil NO_3^- availability for further
365 N_2O production and emission (Zhou et al., 2012; Zhou et al., 2013).

366 Although there were intra- and inter-annual variations in soil N_2O emissions, the soil
367 N_2O flux was significantly affected by soil types throughout the experimental period (Table
368 2). Seasonal cumulative N_2O fluxes from AL were significantly greater than those for AC

369 and NE in wheat seasons, whereas seasonal cumulative N_2O fluxes for AC were
370 significantly greater than for NE and AL in maize seasons. The different soil properties
371 (e.g., pH, clay content, and porosity, Table 1) may have contributed to the significant effects
372 of soil type on N_2O emissions (e.g., reviewed by Butterbach-Bahl et al., 2013; Heil et al.,
373 2015).

374 As soil pH has been shown a key modifier of both biotic and abiotic N transformation
375 processes related to N_2O production and consumption (Butterbach-Bahl et al., 2013; Heil
376 et al., 2015; Wang et al., 2018), the differences in N_2O emissions for the three experimental
377 soils in this study may be related to soil pH. The two years of consecutive observations
378 indicate that the magnitude of N_2O emissions is positively correlated with pH, i.e. that soil
379 N_2O emissions are higher at higher soil pH in the relatively dry and cold wheat season
380 (Table 2). This phenomenon could be explained by the following reasons. First, compared
381 to acidic soils, alkaline soils favor rapid formation of free NH_3, thereby directly providing
382 substrates of ammonia oxidation processes for N_2O production (Kowalchuk and Stephen,
383 2001; Butterbach-Bahl et al., 2013). Second, greater nitrifier functional gene (AOA *amoA,*
384 AOB *amoA,* and *hao*) abundance (Fig. 5) and 2:1 type clay mineral contents (Tables S4
385 and S6) in the neutral and alkaline soils could biologically and physically enhance
386 nitrification rates, thereby increasing soil N_2O production in particular under the aerobic
387 conditions of dry wheat seasons (Butterbach-Bahl et al., 2013; Paustian et al., 2016). Third,
388 N_2O is mainly derived from nitrification at well-aerated, i.e., relatively dry soil conditions
389 (Duan et al., 2018). Similar to our findings, Khan et al. (2011) also detected greater N_2O
390 emissions at higher soil pH from a Paparua Templeton silt loam soil under dry conditions,
391 which was most likely because limitation of N_2O production by low soil moisture

conditions was faster and stronger in acidic soils than in neutral or alkaline soils. In contrast, in wet and warm maize seasons, the current study indicates that soil N_2O emissions from acidic soil tends to be greater than other soil types (Table 2), which is in line with a recent global meta-analysis of soil pH effects on N_2O emissions from agricultural soils (Wang et al., 2018). Some previous studies have also reported negative correlations between soil N_2O emissions and soil pH, i.e. with low pH tending to increase soil N_2O emissions (Liu et al., 2017b; Wang et al., 2018; Shaaban et al, 2018; Wu et al, 2018) (Fig. 4, Fig. 7). For example, the pulses of N_2O emissions following fertilization events in acidic soils were consistently more than two weeks longer than those in high pH soils throughout the whole experimental period (Fig. 3e). These results could be explained by the following mechanisms. First, in warm and wet maize seasons, the average soil NH_4^+ contents for acidic soils (AC treatment: 59.3 mg N kg^{-1}) were significantly higher than those for high pH soils (NE treatment: 12.5 mg N kg^{-1}, AL treatment: 2.5 mg N kg^{-1}) following fertilization events, which in turn increased the availability of soil NH_4^+ for nitrification processes (Figs. 2 and 3). Second, the relatively slow nitrification of acidic soil not only generates N_2O directly but also continuously produces NO_3^- and increases soil NO_3^- availability (mean: 42.3 mg N kg^{-1} for AC, 21.5 mg N kg^{-1} for NE, and 11.8 mg N kg^{-1} for AL), thereby enhancing the denitrification potential, especially in combination with rainfall events (e.g., Butterbach-Bahl et al., 2013). Third, the low *nosZ* gene abundance of AC suggests a decreased activity of N_2O-reductase, and therefore an inhibition of complete denitrification. This will lead to a concomitant increase in the denitrification $N_2O/(N_2O+N_2)$ production ratio, and thus to an increase in soil N_2O emissions (Wu et al., 2018; Shaaban et al., 2018). Soil N_2O emissions are dependent on various biotic and abiotic N

transformation processes that relate to the production and consumption of N_2O in soils, however, the regulating mechanisms of soil pH in these processes are still unclear (Jiang et al., 2015; Liu et al., 2017a), suggesting the need for further targeted study.

In addition to soil pH, soil texture could moderate soil O_2 availability and regulate soil N_2O emissions by impacting the size and distribution of soil pores (Groffman and Tiedje, 1991; Corre et al., 1999; Butterbach-Bahl et al., 2013; Zhou et al., 2017a; Song et al., 2018). In this context, differences in soil texture may be also another explanation for the observed effects of soil type (Tables 1 and 2). Specifically, it is possible that the different clay contents of different soils contributed to the significant effects of soil type on annual N_2O fluxes. This is likely because higher clay particles hold water tightly in soil aggregates and have low gas diffusivity, which might raise the potential for formation of anaerobic microsites, thereby favoring soil N_2O emission from denitrification (Gu et al., 2013). Low soil N_2O emissions at high clay content (> 40%) have often been observed in previous studies, most likely due to low gas diffusivity, which promotes complete denitrification with reduction of N_2O to N_2 (Weitz et al., 2001). Similarly, some studies have highlighted that soil gas diffusivity is a predictable indicator of soil N_2O emission potential (Balaine et al., 2013).

4.2 Temperature sensitivity of N_2O emission

In the present study, soil N_2O emissions increased exponentially with soil temperature in all three soils (Fig. 6), which is consistent with previous field or laboratory studies on various ecosystems (Yao et al. 2010; Song et al. 2018; Zhou et al. 2018; Li et al., 2020). The temperature sensitivity of soil N_2O emission varied substantially among soils, with the

Q_{10} values of soil N_2O emissions ranging from 1.15 to 4.06, which are comparable with values obtained in previous field studies (Smith 1997: 1.5–5.0), as well as in incubation studies (Song et al., 2018: 1.1–5.3). Given the dominance of biological enzymes that catalyze the production of N_2O (Butterbach-Bahl et al., 2013), the temperature dependence of N_2O emissions is understandable because the enzymatic activity generally increases with rising temperature within an appropriate range, as long as no other factors limitations exist. Moreover, the increasing temperature could also physically enhance soil N_2O diffusion and emission processes (Gu et al., 2013; Butterbach-Bahl et al., 2013).

The present study showed that the Q_{10} values of N_2O emissions increased significantly with decreasing soil pH (Fig. S1), which is consistent with recent findings in steppe systems (Zhang et al., 2020). This pattern could be related to the effects of soil pH on the activities of N_2O-generating processes and on the form and availability of the substrate, which then directly/indirectly affecting the Q_{10} of N_2O emissions (Yao et al., 2010; Song et al., 2018). Moreover, it also could be related to a stronger shift from biological N_2O production with lower temperature sensitivity at higher soil pH to more abiotic (chemical) N_2O production with high temperature sensitivity at lower soil pH (Liu et al., 2017a; Liu et al., 2019). The activation energy of specific substrates for N_2O production is relatively stable for the given N_2O production pathways (Butterbach-Bahl et al., 2013; Heil et al., 2015). Thus, the variability of Q_{10} would be decided by the relative proportions as well as the magnitudes of different N_2O production pathways for different soils (Blagodatskaya et al., 2014; Song et al., 2018). Some studies have shown that soil pH may affect the microbial communities and subsequent biogeochemical processes of N_2O production and consumption (Fierer and Jackson, 2006; Nicol et al., 2008). For example, Nicol et al. (2008)

461 and Jiang et al. (2015) reported that the soil pH has an important role in shaping the
462 community structures and abundance of ammonia oxidizers in upland and paddy soils,
463 respectively. Similarly, the current study found that the abundance of functional genes
464 (AOA *amoA,* AOB *amoA, hao, napA, nirS, and nirK*) in soil N_2O emissions is correlated
465 with soil pH (Table S5). In addition, the relatively low but long-lasting nitrification process
466 at low pH soils (i.e., AC soil) not only directly generates N_2O but also produces NO_3^-,
467 thereby increasing soil NO_3^- availability for denitrification and N_2O emissions (Fig. 2). The
468 structural equation model (SEM) analysis explained 95% of the variance in Q_{10} values (Fig.
469 S1), which consequently indicates that soil pH, AOB *amoA* gene abundance, and clay
470 minerals could be the key controlling factors for the thermal sensitivity of N_2O emissions.
471
472 *4.3 Implications and perspectives*
473 A better understanding of the effects of soil type on N_2O emissions via multi-year field
474 measurements can contribute to developing mitigation strategies and improving the
475 accuracy of regional and global N_2O inventories. For example, the acidic soil has been
476 found to be a "hot spot" of N_2O emissions in the summer-maize season due to the warm
477 and wet conditions as compared with the other two soils. Thus, our findings highlight that
478 pH management is crucial for mitigating soil N_2O emissions, in particular for tropical and
479 subtropical regions with widespread acidic soils and wet and warm conditions. For alkaline
480 and neutral soils, the application of nitrification inhibitors could inhibit the ammonia-
481 oxidizing process and reduce N_2O emissions (Tian et al., 2017; Wu et al., 2017),
482 representing an optimal management practice for mitigating soil N_2O emissions because
483 nitrification is the major contributor to soil N_2O emissions in these soils (Tierling and

Kuhlmann, 2018).

In addition, soil types not only control the dynamics and magnitude of N_2O emissions but also regulate the thermal sensitivity (Q_{10}) of soil N_2O emissions. For example, a recent global meta-analysis reported a negative relationship between N_2O emissions and soil pH (Wang et al., 2018), this contrasts with the response pattern of N_2O emissions to soil pH observed in this study, which is likely due to different Q_{10} values among different soils. Thus, soil properties (especially soil pH) should be carefully considered when estimating regional and global N_2O emissions and predicting the response of soil N_2O emissions to climate warming.

5. Conclusion

The results of the present study indicate that soil type plays a crucial role in N_2O emissions in mountain areas. Annual N_2O emissions from acidic soil were significantly greater than for neutral and alkaline soils under identical climate and agricultural management practices. However, the effects of soil pH on N_2O emissions were inconsistent between wheat and maize seasons. The different soil properties, such as soil pH, availability of C and N substrates, and bacterial ammonia monooxygenase gene abundance were the main drivers of the differences in N_2O emissions across different soils. Overall, soil type affects not only the magnitude but also the thermal sensitivity of N_2O emissions. Our findings clarify the concern that effects of soil type on N_2O emissions have to be carefully considered for development of mitigation measure and estimate of regional emissions in mountain areas with inherent spatial heterogeneity of soil type.

Acknowledgments

507 This study was supported by the National Key Research and Development Program
508 (2019YFD1100503), the National Natural Science Foundation of China (Grant No.
509 U20A20107) and the key science and technology project in Sichuan Province
510 (2018SZDZX0025).

511 # References

512 Bakken, L.R., Bergaust, L., Liu, B., Frostegard, A., 2012. Regulation of denitrification at
513 the cellular level: a clue to the understanding of N_2O emissions from soils. Philos.
514 Trans. R. Soc. B-Biol. Sci. 367, 1226-1234. https://doi.org/10.1098/rstb.2011.0321

515 Balaine, N., Clough, T.J., Beare, M.H., Thomas, S.M., Meenken, E.D., Ross, J.G., 2013.
516 Changes in relative gas diffusivity explain soil nitrous oxide flux dynamics. Soil Sci.
517 Soc. Am. J. 77, 1496-1505. https://doi.org/10.2136/sssaj2013.04.0141

518 Blagodatskaya, E., Zheng, X., Blagodatsky, S., Wiegl, R., Dannenmann, M., Butterbach-
519 Bahl, K., 2014. Oxygen and substrate availability interactively control the temperature
520 sensitivity of CO_2 and N_2O emission from soil. Biol. Fertil. Soils 50, 775-783.
521 https://doi.org/10.1007/s00374-014-0899-6

522 Borken, W., Brumme, R., 1997. Liming practice in temperate forest ecosystems and the
523 effects on CO_2, N_2O and CH_4 fluxes. Soil Use Manage. 13, 251-257.
524 https://doi.org/10.1111/j.1475-2743.1997.tb00596.x

525 Butterbach-Bahl, K., Baggs, E.M., Dannenmann, M., Kiese, R., Zechmeister-Boltenstern,
526 S., 2013. Nitrous oxide emissions from soils: how well do we understand the processes
527 and their controls? Philos. Trans. R. Soc. B-Biol. Sci. 368, 20130122.
528 https://doi.org/10.1098/rstb.2013.0122

529 Chirinda N, Carter M.S, Albert K.R, Ambus P, Olesen J.E, Porter J.R, et al. Emissions of
530 nitrous oxide from arable organic and conventional cropping systems on two soil types.
531 Agric. Ecosyst. Environ. 2010; 136: 199-208.
532 https://doi.org/10.1016/j.agee.2009.11.012

533 Corre, M.D., Pennock, D.J., Van Kessel, C., Elliott, D.K., 1999. Estimation of annual

534 nitrous oxide emissions from a transitional grassland-forest region in Saskatchewan,
535 Canada. Biogeochemistry 44, 29-49. https://doi.org/10.1007/bf00992997
536 Davidson, E.A., Matson, P.A., Vitousek, P.M., Riley, R., Dunkin, K., García-Méndez, G.,
537 Maass, J.M., 1993. Processes Regulating Soil Emissions of NO and N_2O in a
538 Seasonally Dry Tropical Forest. Ecology 74, 130-139.
539 https://doi.org/10.2307/1939508
540 Duan, P.P., Wu, Z., Zhang, Q.Q., Fan, C.H., Xiong, Z.Q., 2018. Thermodynamic responses
541 of ammonia-oxidizing archaea and bacteria explain N_2O production from greenhouse
542 vegetable soils. Soil Biol. Biochem. 120, 37-47.
543 https://doi.org/10.1016/j.soilbio.2018.01.027
544 Fierer, N., Jackson, R.B., 2006. The diversity and biogeography of soil bacterial
545 communities. Proc. Natl. Acad. Sci. U. S. A. 103, 626-631.
546 https://doi.org/10.1073/pnas.0507535103
547 Fierer, N., Colman, B.P., Schimel, J.P., Jackson, R.B., 2006. Predicting the temperature
548 dependence of microbial respiration in soil: A continental-scale analysis. Glob.
549 Biogeochem. Cycles 20, 10. https://doi.org/10.1029/2005gb002644
550 Groffman, P.M., Tiedje, J.M., 1991. Relationships between denitrification, CO_2 production
551 and air-filled porosity in soils of different texture and drainage. Soil Biol. Biochem.
552 23, 299-302. https://doi.org/10.1016/0038-0717(91)90067-t
553 Gu, J.X, Zheng, X.H., Wang, Y.H., Ding, W.X., Zhu, B., Chen, X., Wang, Y.Y., Zhao, Z.C.,
554 Shi, Y., Zhu, J.G., 2007. Regulatory effects of soil properties on background N_2O
555 emissions from agricultural soils in China. Plant Soil 295, 53-65.
556 https://doi.org/10.1007/s11104-007-9260-2

557 Gu, J.X., Nicoullaud, B., Rochette, P., Grossel, A., Henault, C., Cellier, P., Richard, G.,
558 2013. A regional experiment suggests that soil texture is a major control of N_2O
559 emissions from tile-drained winter wheat fields during the fertilization period. Soil
560 Biol. Biochem. 60, 134-141. https://doi.org/10.1016/j.soilbio.2013.01.029
561 Heil, J., Liu, S.R., Vereecken, H., Bruggemann, N., 2015. Abiotic nitrous oxide production
562 from hydroxylamine in soils and their dependence on soil properties. Soil Biol.
563 Biochem. 84, 107-115. https://doi.org/10.1016/j.soilbio.2015.02.022IPCC, 2014.
564 Climate Change 2014: Synthesis Report. Contribution of Working Groups I, II and III
565 to the Fifth Assessment Report of the Intergovernmental Panel on Climate Change.
566 IPCC, Geneva, Switzerland, p. 151.
567 Jiang, X.J., Hou, X.Y., Zhou, X., Xin, X.P., Wright, A., Jia, Z.J., 2015. pH regulates key
568 players of nitrification in paddy soils. Soil Biol. Biochem. 81, 9-16.
569 https://doi.org/10.1016/j.soilbio.2014.10.025
570 Khan, S., Clough, T.J., Goh, K.M., Sherlock, R.R., 2011. Influence of soil pH on NO_x and
571 N_2O emissions from bovine urine applied to soil columns. N. Z. J. Agric. Res. 54, 285-
572 301. https://doi.org/10.1080/00288233.2011.607831
573 Kowalchuk, G.A., Stephen, J.R., 2001. Ammonia-oxidizing bacteria: A model for
574 molecular microbial ecology. Annu. Rev. Microbiol. 55, 485-529.
575 https://doi.org/10.1146/annurev.micro.55.1.485
576 Li, L.F., Zheng, Z.Z., Wang, W.J., Biederman, J.A., Xu, X.L., Ran, Q.W., Qian, R.Y., Xu,
577 C., Zhang, B., Wang, F., Zhou, S.T., Cui, L.Z., Che, R.X., Hao, Y.B., Cui, X.Y., Xu,
578 Z.H., Wang, Y.F., 2020. Terrestrial N_2O emissions and related functional genes under
579 climate change: A global meta-analysis. Glob. Change Biol. 26, 931-943.

https://doi.org/10.1111/gcb.14847

Linquist, B., van Groenigen, K.J., Adviento-Borbe, M.A., Pittelkow, C., van Kessel, C., 2012. An agronomic assessment of greenhouse gas emissions from major cereal crops. Glob. Change Biol. 18, 194-209. https://doi.org/10.1111/j.1365-2486.2011.02502.x

Liu, S.R., Han, P., Hink, L., Prosser, J.I., Wagner, M., Bruggemann, N., 2017a. Abiotic Conversion of Extracellular NH_2OH Contributes to N_2O Emission during Ammonia Oxidation. Environ. Sci. Technol. 51, 13122-13132. https://doi.org/10.1021/acs.est.7b02360

Liu, S.R., Schloter, M., Hu, R., Vereecken, H., Brueggemann, N., 2019. Hydroxylamine Contributes More to Abiotic N_2O Production in Soils Than Nitrite. Front. in Environ. Sci. 7, 47. https://doi.org/10.3389/fenvs.2019.00047

Liu, S.W., Lin, F., Wu, S., Ji, C., Sun, Y., Jin, Y.G., Li, S.Q., Li, Z.F., Zou, J.W., 2017b. A meta-analysis of fertilizer-induced soil NO and combined NO+N_2O emissions. Glob. Change Biol. 23, 2520-2532. https://doi.org/10.1111/gcb.13485

Luo, G.J., Brueggemann, N., Wolf, B., Gasche, R., Grote, R., Butterbach-Bahl, K., 2012. Decadal variability of soil CO_2, NO, N_2O, and CH_4 fluxes at the Hoglwald Forest, Germany. Biogeosciences 9, 1741-1763. https://doi.org/10.5194/bg-9-1741-2012

Mctaggart, I.P., Akiyama, H., Tsuruta, H., Ball, B.C., 2002. Influence of soil physical properties, fertiliser type and moisture tension on N_2O and NO emissions from nearly saturated Japanese upland soils. Nutr. Cycl. Agroecosyst. 63, 207-217. https://doi.org/10.1023/A:1021119412863

Nicol, G.W., Leininger, S., Schleper, C., Prosser, J.I., 2008. The influence of soil pH on the diversity, abundance and transcriptional activity of ammonia oxidizing archaea and

603 bacteria. Environ. Microbiol. 10, 2966-2978. https://doi.org/10.1111/j.1462-
604 2920.2008.01701.x
605 Obia, A., Cornelissen, G., Mulder, J., Dorsch, P., 2015. Effect of Soil pH Increase by
606 Biochar on NO, N_2O and N_2 Production during Denitrification in Acid Soils. Plos One
607 10, 19. https://doi.org/10.1371/journal.pone.0138781
608 Parkin, T.B., Kaspar, T.C., 2006. Nitrous oxide emissions from corn-soybean systems in
609 the Midwest. J Environ. Qual. 35, 1496-1506. https://doi.org/10.2134/jeq2005.0183
610 Parkin T, Venterea R.T., 2010. Sampling protocols. Chapter 3. Chamber-based trace gas
611 flux measurements. In: RF F (ed) Sampling protocols. USDA, Mankato.
612 http://www.ars.usda.gov/research/GRACEnet
613 Paustian, K., Lehmann, J., Ogle, S., Reay, D., Robertson, G.P., Smith, P., 2016. Climate-
614 smart soils. Nature 532, 49-57. https://doi.org/10.1038/nature17174
615 Pelster D.E, Chantigny M.H, Rochette P, Angers D.A, Rieux C, Vanasse A., 2012. Nitrous
616 Oxide Emissions Respond Differently to Mineral and Organic Nitrogen Sources in
617 Contrasting Soil Types. J Environ. Qual. 41, 427-435.
618 https://doi.org/10.2134/jeq2011.0261
619 Pilegaard, K., 2013. Processes regulating nitric oxide emissions from soils. Philos. Trans.
620 R. Soc. B-Biol. Sci. 368, 20130126. https://doi.org/10.1098/rstb.2013.0126
621 Rowlings, D.W., Grace, P.R., Kiese, R., Weier, K.L., 2012. Environmental factors
622 controlling temporal and spatial variability in the soil-atmosphere exchange of CO_2,
623 CH_4 and N_2O from an Australian subtropical rainforest. Glob. Change Biol. 18, 726-
624 738. https://doi.org/10.1111/j.1365-2486.2011.02563.x
625 Schindlbacher, A., Zechmeister-Boltenstern, S., Butterbach-Bahl, K., 2004. Effects of soil

626 moisture and temperature on NO, NO_2, and N_2O emissions from European forest soils.
627 J. Geophys. Res. 109. https://doi.org/10.1029/2004jd004590
628 Shaaban, M., Wu, Y.P., Khalid, M.S., Peng, Q.A., Xu, X.Y., Wu, L., Younas, A., Bashir, S.,
629 Mo, Y.L., Lin, S., Zafar-ul-Hye, M., Abid, M., Hu, R.G., 2018. Reduction in soil N_2O
630 emissions by pH manipulation and enhanced *nosZ* gene transcription under different
631 water regimes. Environ. Pollut. 235, 625-631.
632 https://doi.org/10.1016/j.envpol.2017.12.066
633 Shang, Z.Y., Abdalla, M., Kuhnert, M., Albanito, F., Zhou, F., Xia, L.L., Smith, P., 2020.
634 Measurement of N_2O emissions over the whole year is necessary for estimating
635 reliable emission factors. Environ. Pollut. 259, 113864.
636 https://doi.org/10.1016/j.envpol.2019.113864
637 Shcherbak, I., Millar, N., Robertson, G.P., 2014. Global metaanalysis of the nonlinear
638 response of soil nitrous oxide (N_2O) emissions to fertilizer nitrogen. Proc. Natl. Acad.
639 Sci. U. S. A. 111, 9199-9204. https://doi.org/10.1073/pnas.1322434111
640 Skiba, U., Ball, B., 2002. The effect of soil texture and soil drainage on emissions of nitric
641 oxide and nitrous oxide. Soil Use Manage. 18, 56-60. https://doi.org/10.1111/j.1475-
642 2743.2002.tb00050.x
643 Smith, K.A., Mctaggart, I.P., Tsuruta, H., 1997. Emissions of N_2O and NO associated with
644 nitrogen fertilization in intensive agriculture, and the potential for mitigation. Soil Use
645 Manage. 13, 296-304. https://doi.org/10.1111/j.1475-2743.1997.tb00601.x
646 Song, A.L., Liang, Y.C., Zeng, X.B., Yin, H.Q., Xu, D.Y., Wang, B.R., Wen, S.L., Li, D.C.,
647 Fan, F.L., 2018. Substrate-driven microbial response: A novel mechanism contributes
648 significantly to temperature sensitivity of N_2O emissions in upland arable soil. Soil

649 Biol. Biochem. 118, 18-26. https://doi.org/10.1016/j.soilbio.2017.11.021
650 Song, X.T., Ju, X.T., Topp, C.F.E., Rees, R.M., 2019. Oxygen Regulates Nitrous Oxide
651 Production Directly in Agricultural Soils. Environ. Sci. Technol. 53, 12539-12547.
652 https://doi.org/10.1021/acs.est.9b03089
653 Stevens, R.J., Laughlin, R.J., Malone, J.P., 1998. Soil pH affects the processes reducing
654 nitrate to nitrous oxide and di-nitrogen. Soil Biol. Biochem. 30, 0-1126.
655 https://doi.org/10.1016/s0038-0717(97)00227-7
656 Szukics, U., Abell, G.C.J., Hödl, V., Mitter, B., Sessitsch, A., Hackl, E.,
657 Zechmeisterboltenstern, S., 2010. Nitrifiers and denitrifiers respond rapidly to
658 changed moisture and increasing temperature in a pristine forest soil. FEMS Microbiol.
659 Ecol. 72, 395–406. https://doi.org/10.1111/j.1574-6941.2010.00853.x
660 Tian, D., Zhang, Y.Y., Zhou, Y.Z., Mu, Y.J., Liu, J.F., Zhang, C.L., Liu, P.F., 2017. Effect
661 of nitrification inhibitors on mitigating N_2O and NO emissions from an agricultural
662 field under drip fertigation in the North China Plain. Sci. Total Environ. 598, 87-96.
663 https://doi.org/10.1016/j.scitotenv.2017.03.220
664 Tierling, J., Kuhlmann, H., 2018. Emissions of nitrous oxide (N_2O) affected by pH-related
665 nitrite accumulation during nitrification of N fertilizers. Geoderma 310, 12-21.
666 https://doi.org/10.1016/j.geoderma.2017.08.040
667 Wang, Y.J., Guo, J.H., Vogt, R.D., Mulder, J., Wang, J.G., Zhang, X.S., 2018. Soil pH as
668 the chief modifier for regional nitrous oxide emissions: New evidence and
669 implications for global estimates and mitigation. Glob. Change Biol. 24, e617-e626.
670 https://doi.org/10.1111/gcb.13966
671 Weitz, A.M., Linder, E., Frolking, S., Crill, P.M., Keller, M., 2001. N_2O emissions from

672 humid tropical agricultural soils: effects of soil moisture, texture and nitrogen
673 availability. Soil Biol. Biochem. 33, 1077-1093. https://doi.org/10.1016/s0038-
674 0717(01)00013-x
675 Wu, D., Cardenas, L.M., Calvet, S., Bruggemann, N., Loick, N., Liu, S.R., Bol, R., 2017.
676 The effect of nitrification inhibitor on N_2O, NO and N_2 emissions under different soil
677 moisture levels in a permanent grassland soil. Soil Biol. Biochem. 113, 153-160.
678 https://doi.org/10.1016/j.soilbio.2017.06.007
679 Wu, D., Senbayram, M., Zang, H.D., Ugurlar, F., Aydemir, S., Bruggemann, N., Kuzyakov,
680 Y., Bol, R., Blagodatskaya, E., 2018. Effect of biochar origin and soil pH on
681 greenhouse gas emissions from sandy and clay soils. Appl. Soil Ecol. 129, 121-127.
682 https://doi.org/10.1016/j.apsoil.2018.05.009
683 Yao, Z.S., Wu, X., Wolf, B., Dannenmann, M., Butterbach-Bahl, K., Brüggemann, N.,
684 Chen, W.W., Zheng, X.H, 2010. Soil-atmosphere exchange potential of NO and N_2O
685 in different land use types of Inner Mongolia as affected by soil temperature, soil
686 moisture, freeze-thaw, and drying-wetting events. J. Geophys. Res. 115.
687 https://doi.org/10.1029/2009JD013528
688 Yao, Z.S., Liu, C.Y., Dong, H.B., Wang, R., Zheng, X.H., 2015. Annual nitric and nitrous
689 oxide fluxes from Chinese subtropical plastic greenhouse and conventional vegetable
690 cultivations. Environ. Pollut. 196, 89-97.
691 https://doi.org/10.1016/j.envpol.2014.09.010
692 Zhang, H.J., Yao, X., Zeng, W., Fang, Y., Wang, W., 2020. Depth dependence of
693 temperature sensitivity of soil carbon dioxide, nitrous oxide and methane emissions.
694 Soil Biol. Biochem. 149, 107956. https://doi.org/10.1016/j.soilbio.2020.107956

695 Zhou, M.H., Zhu, B., Butterbach-Bahl, K., Wang, T., Bergmann, J., Brueggemann, N.,
696 Wang, Z.H., Li, T.K., Kuang, F.H., 2012. Nitrate leaching, direct and indirect nitrous
697 oxide fluxes from sloping cropland in the purple soil area, southwestern China.
698 Environ. Pollut. 162, 361-368. https://doi.org/10.1016/j.envpol.2011.12.001
699 Zhou, M.H., Zhu, B., Butterbach-Bahl, K., Zheng, X.H., Wang, T., Wang, Y.Q., 2013.
700 Nitrous oxide emissions and nitrate leaching from a rain-fed wheat-maize rotation in
701 the Sichuan Basin, China. Plant Soil 362, 149-159. https://doi.org/10.1007/s11104-
702 012-1269-5
703 Zhou, M.H., Wang, X.G., Wang, Y.Q., Zhu, B., 2018. A three-year experiment of annual
704 methane and nitrous oxide emissions from the subtropical permanently flooded rice
705 paddy fields of China: Emission factor, temperature sensitivity and fertilizer nitrogen
706 effect. Agric. For. Meteorol. 250, 299-307.
707 https://doi.org/10.1016/j.agrformet.2017.12.265
708 Zhou, M.H., Zhu, B., Brueggemann, N., Bergmann, J., Wang, Y.Q., Butterbach-Bahl, K.,
709 2014a. N_2O and CH_4 Emissions, and NO_3^- Leaching on a Crop-Yield Basis from a
710 Subtropical Rain-fed Wheat-Maize Rotation in Response to Different Types of
711 Nitrogen Fertilizer. Ecosystems 17, 286-301. https://doi.org/10.1007/s10021-013-
712 9723-7
713 Zhou, M.H, Zhu, B., Wang, X.G., Wang, Y.Q., 2017a. Long-term field measurements of
714 annual methane and nitrous oxide emissions from a Chinese subtropical wheat-rice
715 rotation system. Soil Biol. Biochem. 115, 21-34.
716 https://doi.org/10.1016/j.soilbio.2017.08.005
717 Zhou, M.H, Zhu, B., Wang, S.J., Zhu, X.Y., Vereecken, H., Brueggemann, N., 2017b.

718 Stimulation of N_2O emission by manure application to agricultural soils may largely
719 offset carbon benefits: a global meta-analysis. Glob. Change Biol. 23, 4068-4083.
720 https://doi.org/10.1111/gcb.13648
721 Zhu, B., Wang, T., You, X., Gao, M.R., 2008. Nutrient release from weathering of purplish
722 rocks in the Sichuan Basin, China. Pedosphere 18, 257-264.
723 https://doi.org/10.1016/s1002-0160(08)60015-6
724 Zhu G.D, Song X.T, Ju X.T, Zhang J.B, Muller C, Sylvester-Bradley R, et al. Gross N
725 transformation rates and related N_2O emissions in Chinese and UK agricultural soils.
726 Sci. Total Environ. 2019; 666: 176-186. https://doi.org/
727 10.1016/j.scitotenv.2019.02.241

Figure. 1 Temporal dynamics of (a) daily maximum (Max AT), minimum (Min AT) air temperature, daily precipitation and soil (10 cm) temperature of AC, NE and AL soils, and (b) water filled pore space (WFPS) of AC, NE and AL. AC, NE and AL indicate the acidic, neutral and alkaline soil types, respectively.

Figure. 2 Box-whisker plots of (a) soil temperature, (b) soil WFPS, (c) ammonium (NH_4^+), (d) nitrate (NO_3^-), (e) nitrite (NO_2^-), (f) dissolved organic carbon (DOC) concentrations and (e) nitrous oxide (N_2O) emission rate of different soil types in the wheat and maize seasons. In box-whisker plots, the top edges of the box indicate the 25th and 75th percentiles, the central line indicates the median, and the square white dots indicate the average, respectively. The maximum whisker lengths are specified as 1.5 times the interquartile range. Different letters mean significant differences among soils in the wheat and maize seasons (p<0.05, one-way ANOVA, post-hoc LSD test). SDW is soil dry weight. AC, NE and AL indicate the acidic, neutral and alkaline soil types, respectively.

Figure. 3 Temporal dynamics of topsoil (0-15cm) (a) ammonium (NH_4^+), (b) nitrate (NO_3^-), (c) nitrite (NO_2^-), (d) dissolved organic carbon (DOC) content and (e) soil nitrous oxide (N_2O) emission rates of different soil types for the wheat-maize rotation system. The data shown in all panels are average and standard error of four spatial replicates for each soil type. The black downward arrows indicate the fertilization date. SDW is soil dry weight. AC, NE and AL indicate the acidic, neutral and alkaline soil types, respectively.

Figure. 4 Temporal cumulative N_2O emissions (kg N ha^{-1}) from the different soils during 2017-2018 (a) and 2018-2019 (b). The data shown in all panels are average and standard

error of four spatial replicates for each soil type. The black downward arrows indicate the fertilization date. AC, NE and AL indicate the acidic, neutral and alkaline soil types, respectively.

Figure. 5 Functional gene abundance (copies g^{-1} SDW) in the topsoil (0-15 cm) for the nitrification processes (a) (AOA *amoA,* AOB *amoA, hao*) and for the denitrification processes (b) (*narG, napA, nirS, nirK and nosZ*) . Vertical bars indicate standard errors of four replicates. Different letters denote significant differences between soil types (p<0.05). SDW is soil dry weight. AC, NE and AL indicate the acidic, neutral and alkaline soil types, respectively.

Figure. 6 Relationships between N_2O emissions and topsoil temperature for the AC, NE and AL soils throughout the experimental periods of 2017-2019. AC, NE and AL indicate the acidic, neutral and alkaline soil types, respectively.

Figure. 7 Relationships between soil pH and cumulative N_2O [wheat season (a), maize season (b) and annual (c)] emissions from 2017 to 2019.

Figure. 1

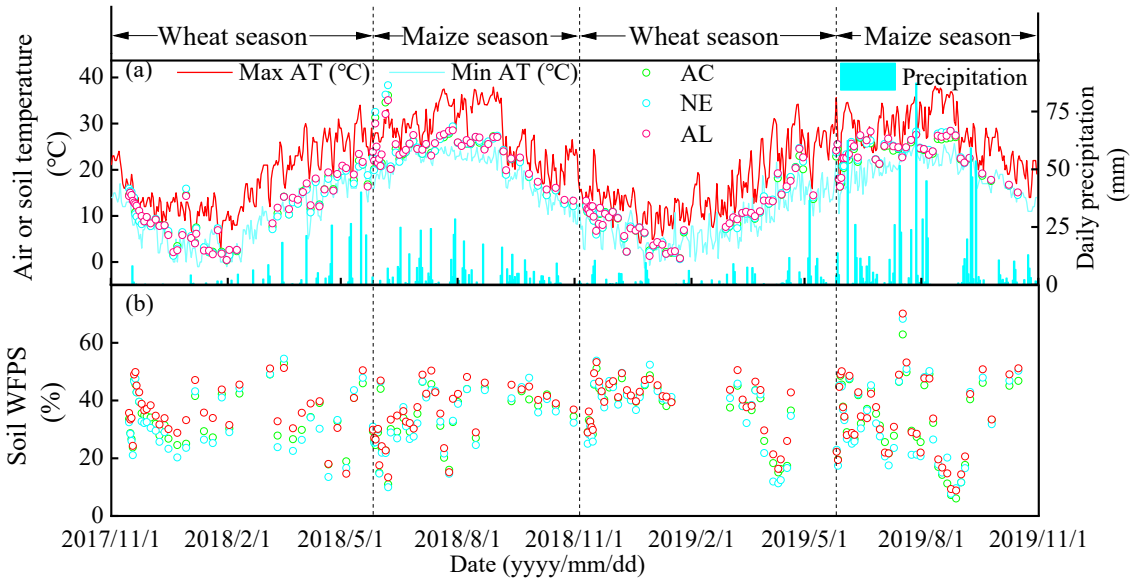
Wheat season
Maize season
Wheat season
Maize season
(a)
Max AT (℃)
Min AT (℃)
AC
NE
AL
Precipitation
Air or soil temperature (℃)
Daily precipitation (mm)
(b)
Soil WFPS (%)
2017/11/1
2018/2/1
2018/5/1
2018/8/1
2018/11/1
2019/2/1
2019/5/1
2019/8/1
2019/11/1
Date (yyyy/mm/dd)

Figure. 2

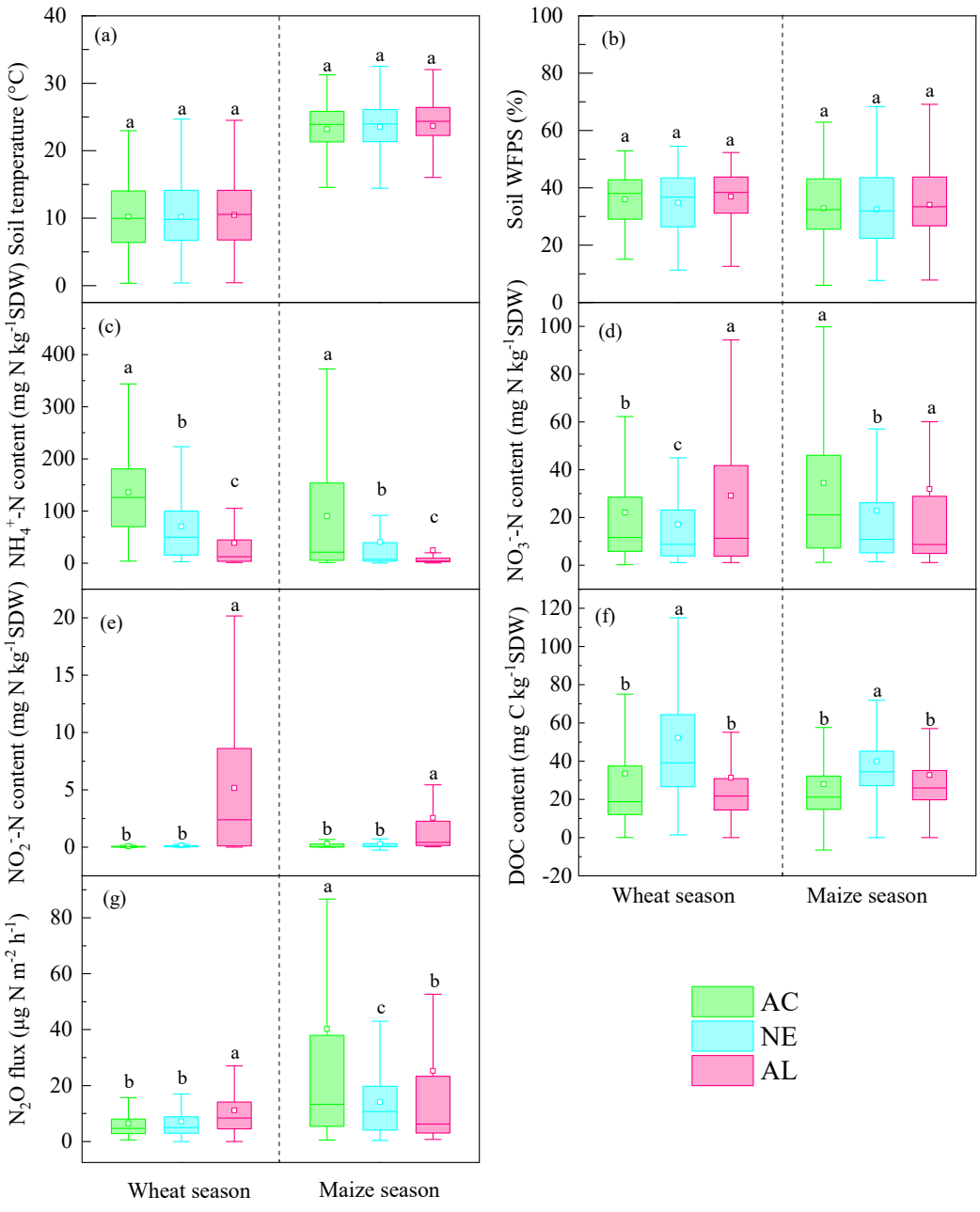
(a)
(b)
(c)
(d)
(e)
(f)
(g)
Soil temperature (°C)
Soil WFPS (%)
NH4+-N content (mg N kg-1SDW)
NO3--N content (mg N kg-1SDW)
NO2--N content (mg N kg-1SDW)
DOC content (mg C kg-1SDW)
N2O flux (μg N m-2 h-1)
Wheat season
Maize season
AC
NE
AL

Figure. 3

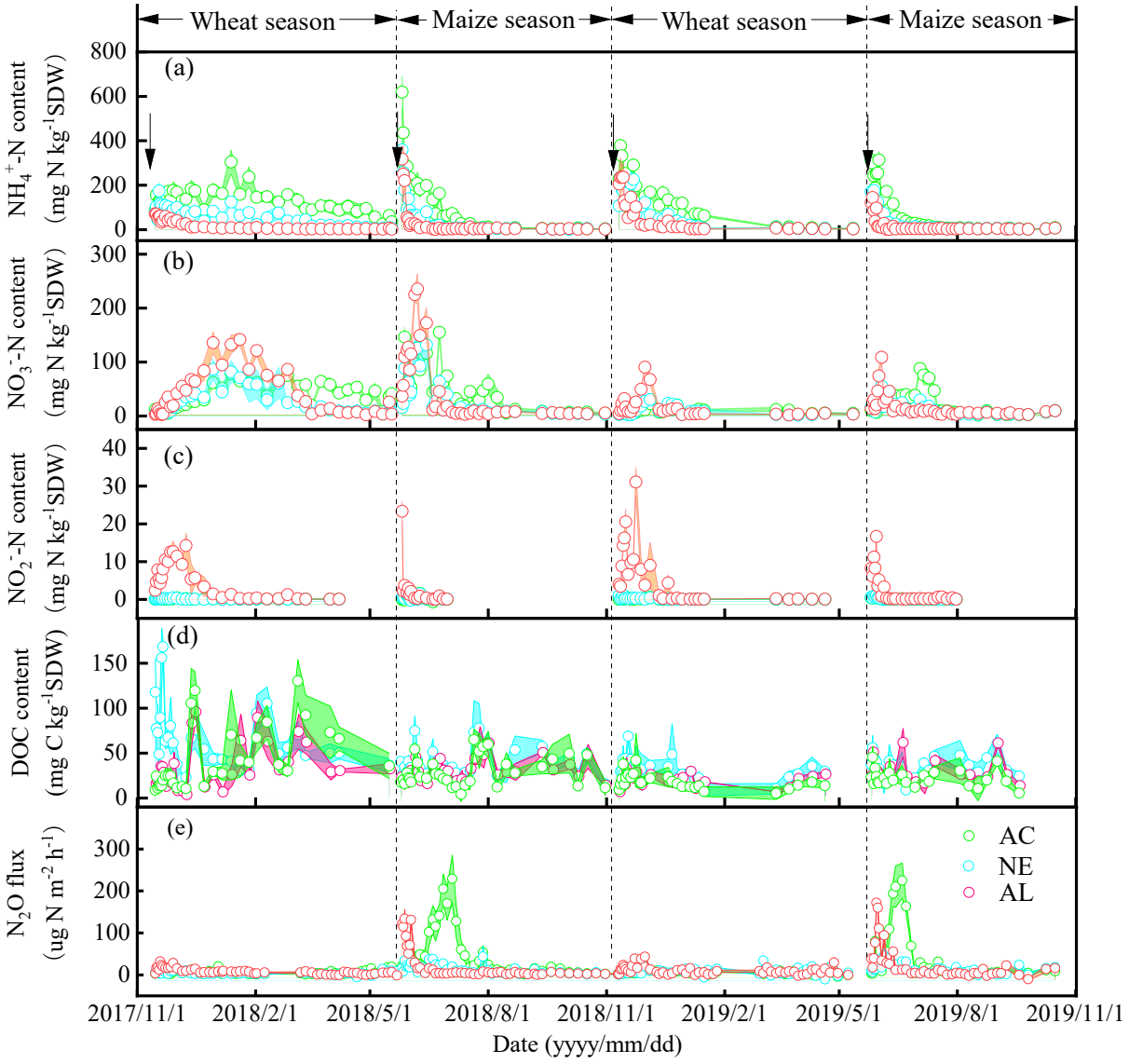
Wheat season
Maize season
Wheat season
Maize season
(a)
NH_4^+-N content (mg N kg^{-1}SDW)
800
600
400
200
0
(b)
NO_3^--N content (mg N kg^{-1}SDW)
300
200
100
0
(c)
NO_2^--N content (mg N kg^{-1}SDW)
40
30
20
10
0
(d)
DOC content (mg C kg^{-1}SDW)
150
100
50
0
(e)
N_2O flux (ug N m^{-2} h^{-1})
300
200
100
0
AC
NE
AL
2017/11/1
2018/2/1
2018/5/1
2018/8/1
2018/11/1
2019/2/1
2019/5/1
2019/8/1
2019/11/1
Date (yyyy/mm/dd)

Figure. 4

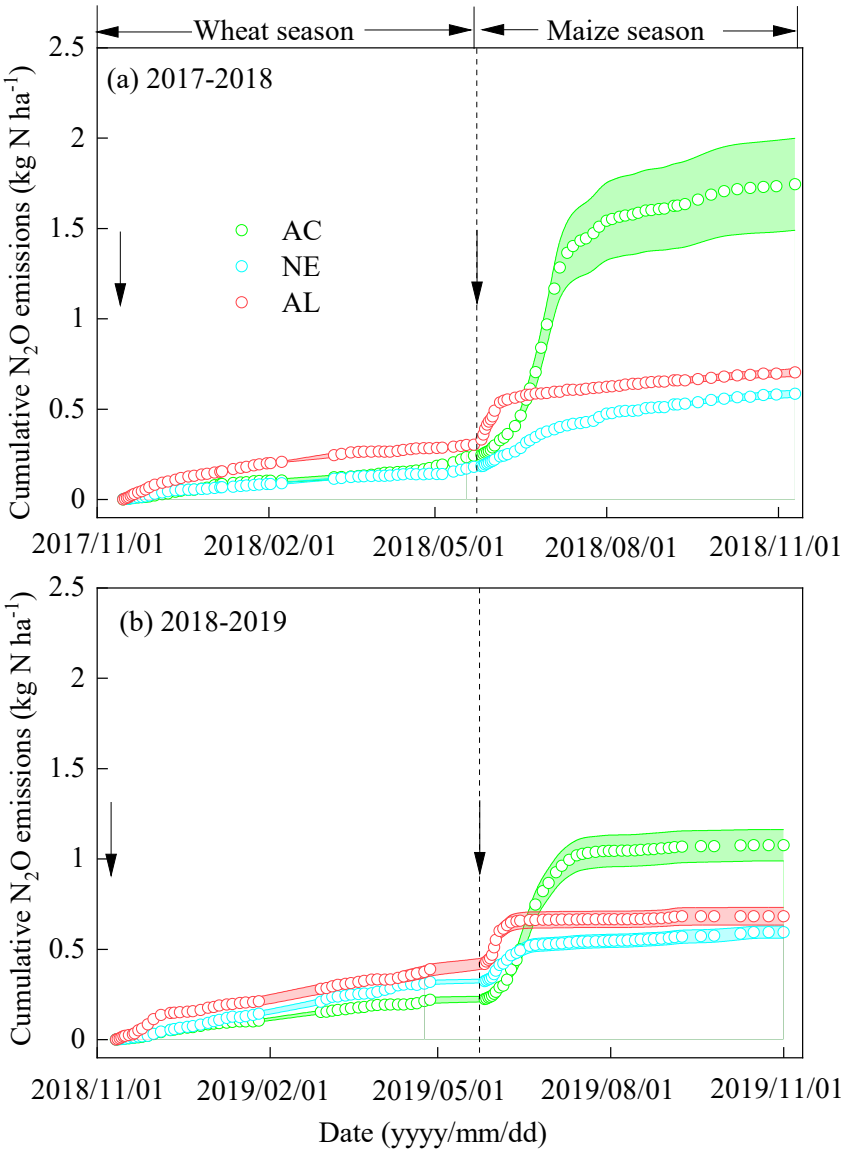
Wheat season
Maize season
(a) 2017-2018
AC
NE
AL
Cumulative N_2O emissions (kg N ha^{-1})
2.5
2
1.5
1
0.5
0
2017/11/01
2018/02/01
2018/05/01
2018/08/01
2018/11/01
(b) 2018-2019
2018/11/01
2019/02/01
2019/05/01
2019/08/01
2019/11/01
Date (yyyy/mm/dd)

Figure. 5

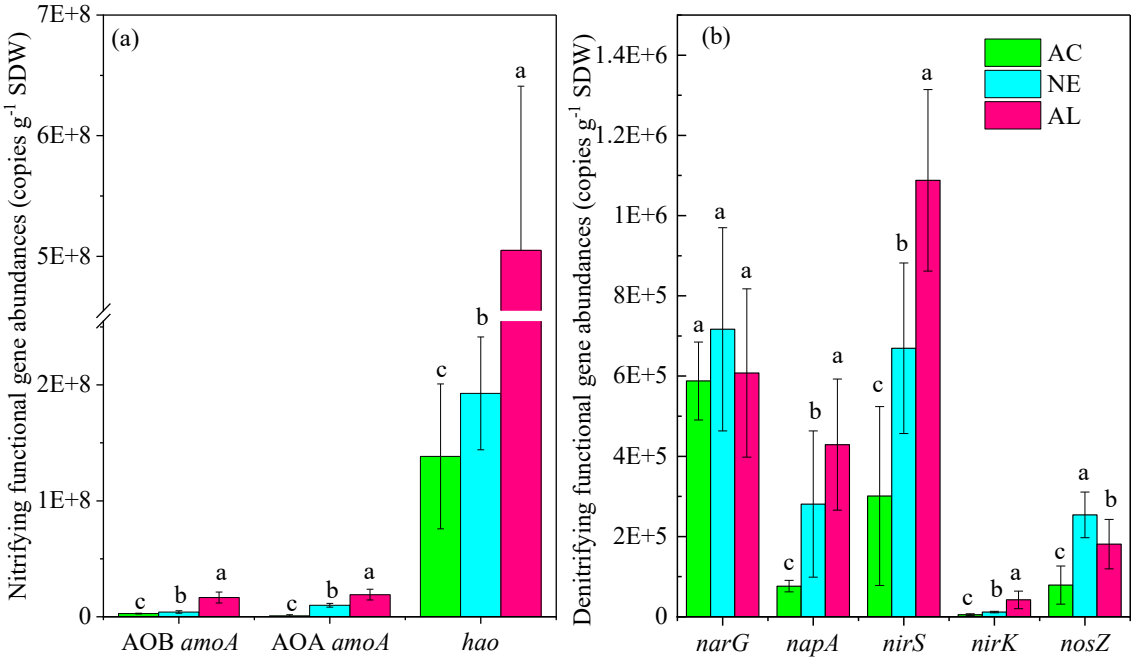
(a)
Nitrifying functional gene abundances (copies g-1 SDW)
7E+8
6E+8
5E+8
2E+8
1E+8
0
c
b
a
c
b
a
c
b
a
AOB amoA
AOA amoA
hao
(b)
Denitrifying functional gene abundances (copies g-1 SDW)
1.4E+6
1.2E+6
1E+6
8E+5
6E+5
4E+5
2E+5
0
AC
NE
AL
narG
napA
nirS
nirK
nosZ

Figure. 6

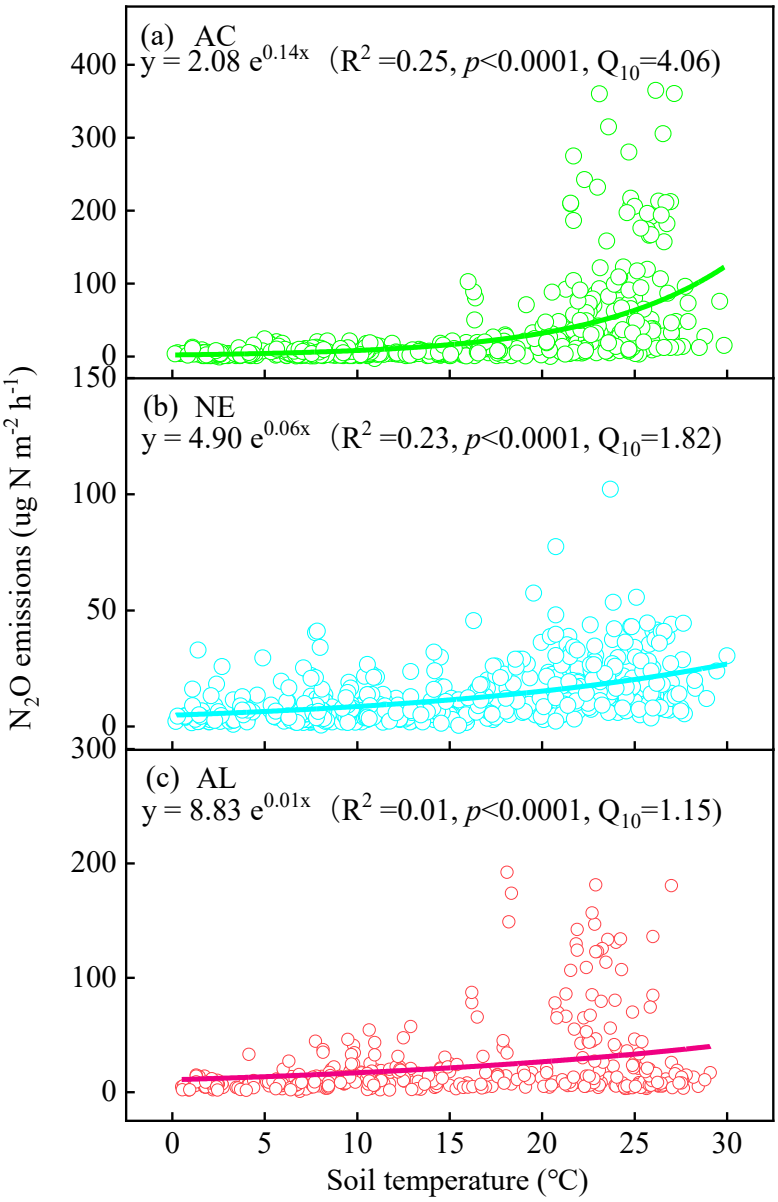
(a) AC
y = 2.08 e^0.14x (R2 =0.25, p<0.0001, Q10=4.06)
(b) NE
y = 4.90 e^0.06x (R2 =0.23, p<0.0001, Q10=1.82)
(c) AL
y = 8.83 e^0.01x (R2 =0.01, p<0.0001, Q10=1.15)
N2O emissions (ug N m-2 h-1)
Soil temperature (℃)

Figure. 7

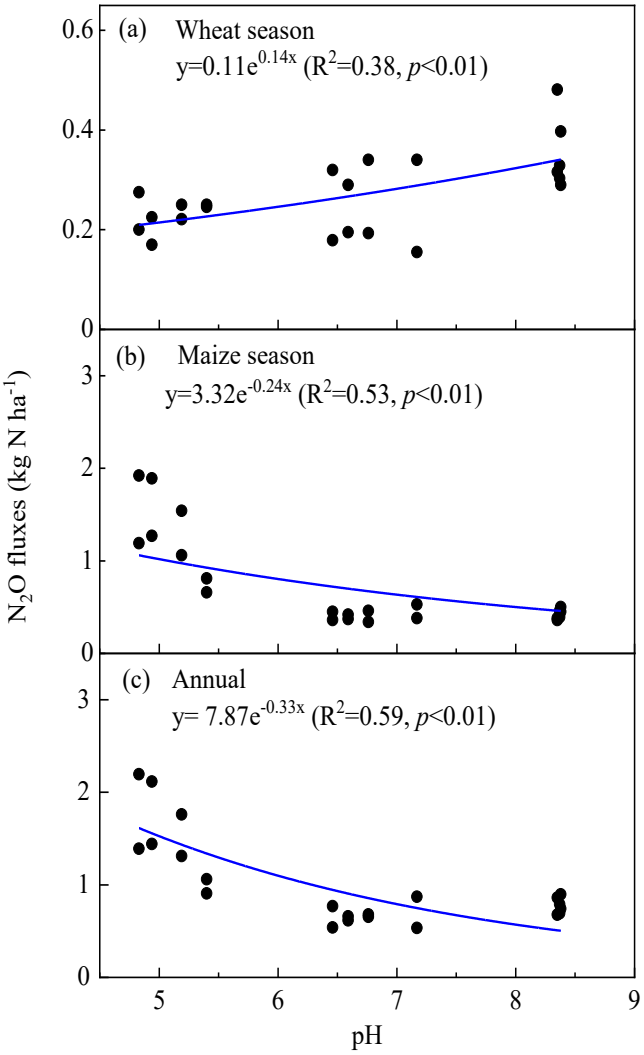
(a) Wheat season
y=0.11e^0.14x (R^2=0.38, p<0.01)
(b) Maize season
y=3.32e^-0.24x (R^2=0.53, p<0.01)
(c) Annual
y= 7.87e^-0.33x (R^2=0.59, p<0.01)
N2O fluxes (kg N ha^-1)
pH
0
0.2
0.4
0.6
1
2
3
5
6
7
8
9

Table 1

Soil pH, soil organic carbon (SOC), total nitrogen (TN), C/N ratio, cation exchange capacity (CEC), bulk density (BD), porosity, texture (clay, silt and sand content), available Fe (DTPA-Fe), available manganese (DTPA-Mn) of the topsoil (0-20 cm).

Soil type	pH	SOC	TN	C/N ratio	CEC	BD	Porosity	Clay	Silt	Sand	Available Fe	Available Mn
		g/kg	g/kg		cmol(+)/kg	g/cm^3	%	%	%	%	mg/kg	mg/kg
AC	5.09±0.11c	6.32±0.41a	0.87±0.01a	21.78±1.22b	2.48±0.09e	0.97±0.02b	59.40±0.75a	32.79±0.35a	50.52±1.24a	16.69±1.13b	0.51±0.05b	21.31±0.80b
NE	6.75±0.13b	5.70±0.29a	0.66±0.02b	25.94±1.27a	8.55±0.02c	1.17±0.03a	53.65±0.86b	17.86±0.68c	53.10±2.05a	29.04±1.61a	0.75±0.11a	22.92±0.43a
AL	8.37±0.01a	5.80±0.09a	0.80±0.03a	21.65±0.99b	8.22±0.09c	1.14±0.01a	53.89±0.73b	30.82±0.31b	51.76±1.87a	17.42±2.13b	0.54±0.08b	6.45±0.84c

Different letters within the same column indicate significant differences among treatments at $p<0.05$ level. AC, NE and AL indicate the acidic, neutral and alkaline soil types, respectively.

Table 2

Seasonal N_2O flux, grain yield, plant N uptake and yield-scaled N_2O emissions in the wheat-maize rotation system.

Soil type	Wheat season				Maize season				Annual			
	N_2O flux (kg N ha^{-1})	Grain yield (Mg ha^{-1})	Plant N uptake (kg N ha^{-1})	Yield-scaled N_2O (g N_2O-N Mg^{-1})	N_2O flux (kg N ha^{-1})	Grain yield (Mg ha^{-1})	Plant N uptake (kg N ha^{-1})	Yield-scaled N_2O (g N_2O-N Mg^{-1})	N_2O flux (kg N ha^{-1})	Grain yield (Mg ha^{-1})	Plant N uptake (kg N ha^{-1})	Yield-scaled N_2O (g N_2O-N Mg^{-1})
2018												
AC	0.24±0.01b	2.6±0.1b	73.5±2.6b	91.4±5.5a	1.50±0.25a	3.3±0.3b	99.1±5.4c	463.8±87.1a	1.74±0.26 a	5.6±0.4b	175.5±13.9b	581.3±96.8a
NE	0.18±0.01c	3.3±0.1a	100.0±16.1a	54.5±3.8b	0.41±0.02b	5.2±0.3a	131.1±6.5a	77.4±0.9b	0.59±0.03 b	8.6±0.2 a	243.8±10.3a	132.1±3.3b
AL	0.30±0.01a	3.1±0.1a	90.4±6.2a	98.9±5.4a	0.40±0.02b	5.2±0.2a	113.4±4.7b	77.2±1.6b	0.70±0.02 b	8.3±0.3a	212.0±6.1ab	176.0±4.1b
2019												
AC	0.22±0.03c	2.9±0.1b	89.2±3.6b	73.9±6.1c	1.08±0.09a	4.7±0.1b	140.2±3.9a	230.1±21.6a	1.30±0.07 a	7.7±0.1b	253.8±5.5 a	301.0±17.0a
NE	0.32±0.02b	3.3±0.04a	102.2±5.5a	99.5±4.0b	0.42±0.04b	5.7±0.04a	132.3±3.6b	74.8±7.0c	0.75±0.04 b	8.9±0.1a	250.2±3.5a	174.3±9.4c
AL	0.40±0.06a	2.9±0.03b	99.0±2.9a	139.1±12.1a	0.45±0.03b	4.4±0.1c	96.7±4.5c	100.2±3.8b	0.85±0.03 b	7.3±0.1b	225.5±8.2b	239.3±10.2b
Source of variance												
Year	**	NS	NS	**	NS	NS	NS	**	NS	*	**	NS
Soil type	**	**	*	**	**	**	**	**	**	**	**	**
Year×soil type	**	NS	**	NS	**	**	*	**	NS	**	**	**

Different letters within the same column indicate significant differences among treatments at $p<0.05$ level. NS indicates not significant; ** and * indicate significant at $p<0.01$ and $p<0.05$ level, respectively. AC, NE and AL indicate the acidic, neutral and alkaline soil types, respectively.

Table 3

Results of linear regression analysis of the effects of soil moisture (WFPS, in %), soil temperature (ST, in ℃), mineral nitrogen substrate ($MN=NH_4^+ + NO_3^- + NO_2^-$) and soil DOC content on N_2O emissions from the AC, NE and AL soil throughout the experimental periods of 2017-2019.

Season	Soil type	Regression function	R^{2a}	p^b	n[c]
Wheat season	AC	$Ln(N_2O) = 0.33ST+0.24WFPS+0.20Ln(MN)-0.15Ln(DOC)-0.66$	0.15	<0.05	185
	NE	$Ln(N_2O) = 0.27Ln(MN)+0.15WFPS+1.96$	0.09	<0.05	193
	AL	$Ln(N_2O) = 0.37Ln(MN)+1.22$	0.13	<0.001	176
Maize season	AC	$Ln(N_2O) = 0.49Ln(MN)+0.33WFPS+0.29ST -2.74$	0.35	<0.001	212
	NE	$Ln(N_2O) = 0.47Ln(MN)+0.39WFPS+0.20ST-1.16$	0.27	<0.001	208
	AL	$Ln(N_2O) = 0.77Ln(MN)+0.25WFPS -1.63$	0.51	<0.001	202
Year-round	AC	$Ln(N_2O) = 0.72ST+0.33Ln(MN)+0.28WFPS -3.08$	0.49	<0.001	391
	NE	$Ln(N_2O) = 0.50ST+0.30WFPS+0.22Ln(MN)-0.16Ln(DOC)+0.29$	0.26	<0.001	382
	AL	$Ln(N_2O) = 0.62Ln(MN)+0.22ST+0.20WFPS-1.27$	0.34	<0.001	391

[a] Coefficient of determination; [b] Level of significance; [c] the symbol "n" represents the number of measurements. AC, NE and AL indicate the acidic, neutral and alkaline soil types, respectively.